2D and 3D Maximum-Quantum NMR and diffusion spectroscopy for the characterization of enzymatic reaction mixtures

Elena Piersanti, Claudio Righetti, David Ribeaucourt, A. Jalila Simaan, Yasmina Mekmouche, Mickael Lafond, Jean-Guy Berrin, Thierry Tron, Mehdi Yemloul

Analyst

Accepted Manuscript

This article can be cited before page numbers have been issued, to do this please use: E. Piersanti, C. Righetti, D. Ribeaucourt, A. J. Simaan, Y. Mekmouche, M. Lafond, J. Berrin, T. Tron and M. Yemloul, *Analyst*, 2022, DOI: 10.1039/D2AN00200K.

ROYAL SOCIETY OF CHEMISTRY

rsc.li/analyst

View Article Online
DOI: 10.1039/D2AN00200K

ARTICLE

2D and 3D Maximum-Quantum NMR and diffusion spectroscopy for the characterization of enzymatic reaction mixtures

Received 00th January 20xx,
Accepted 00th January 20xx

DOI: 10.1039/x0xx00000x

Elena Piersanti[a], Claudio Righetti[a], David Ribeaucourt[a,b,c], A. Jalila Simaan[a], Yasmina Mekmouche[a], Lafond Mickael[a], Jean-Guy Berrin[b], Thierry Tron[a] and Mehdi Yemloul[a*]

1D ^{1}H NMR spectroscopy has been widely used to monitor enzymatic activity by recording the evolution of the spectra of substrates and/or products thanks to the linear response of NMR. For complex systems involving the coexistence of multiple compounds (substrate, final product and various intermediates), the identification and quantification can be a more arduous task. Here, we present a simple analytical method for a rapid characterization of reaction mixtures involving enzymatic complexes using Maximum Quantum (MaxQ) NMR, accelerated with the Non-Uniform Sampling (NUS) acquisition procedure. Specifically, this approach enables, in a first analytical step, to count the molecules present in the samples. We also show, using two different enzymatic systems, that the implementation of these pulse sequences implies precautions related to the short relaxation times due to the presence of metallo-enzymes or paramagnetic catalysts. Finally, the combination of MaxQ and diffusion experiments, which leads to a 3D chart, greatly improves the resolution and offers an extreme simplification of the spectra while giving valuable indications on the affinity of the enzymes to the different compounds present in the reaction mixture.

Introduction

Nuclear Magnetic Resonance (NMR) has been widely used to characterize enzymatic processes that are complex, dynamic and time-dependent. Thanks to the quantitative linear response, one dimensional (1D) ^{1}H and hetero-nuclei (^{13}C, ^{31}P, ^{19}F...)[1 2] NMR have been the most used to record the delicate and fast variations in concentrations of substrates and products as a function of time.[3 4] The methodological developments associated with recent studies have undergone a significant renewal and provided versatile protocols, as the real-time NMR experiments,[5 6 7] to monitor in a fast and reproducible manner enzyme kinetics and to estimate, under favourable conditions, the Michaelis constant.[8] Other methods have been developed to carry out studies close to real conditions with the so-called in-cell NMR. As an example, 1D ^{1}H spectra were used to monitor the hydrolytic decomposition of the carbapenem antibiotic meropenem inside *Escherichia coli* cells.[4] In general, the effective use of quantitative ^{1}H NMR depends on the speciation of one or several well-defined peaks from crowded spectra for each component in the reaction mixture, even if the information have to be extracted from overlapping peaks. In this context, the contribution of NMR methods designed for mixture analyses are valuable and obvious. The most common NMR techniques used for mixture analysis are TOtal Correlation SpectroscopY (TOCSY) and Diffusion Ordered SpectroscopY (DOSY) that brings the closest similarity to chromatography. In this experiment, molecules are labeled by their molecular diffusion, which is roughly determined by the molecular size.[9] Thus, the spectra of the components can be extracted if the differences in the molecular diffusions are large enough.[10 1 11 12 13 14] Otherwise the resolving power of DOSY will be restricted.[15] Three-dimensional NMR sequences aiming at increasing the resolving power of DOSY through a third dimension have been developed to resolve overlapping resonances.[16 17 18 19 20] However, a wide use of these methods has been thwarted due to the long acquisition time required for recording several dimensions. Recently, the suitability of ^{1}H Maximum-Quantum NMR for mixture analysis was demonstrated, providing a higher resolution, in favorable cases, up to tens of molecules.[21] Maximum-Quantum NMR is a 2D experiment that can be considered as providing the joint information of DOSY and TOCSY. Indeed, 2D MaxQ-NMR aims at isolating the NMR signal belonging to a same molecular fragment, carrying at least a specific number of protons, *p*, in a way similar to TOCSY. The information is then simplified as in the indirect dimension, all of these signals contribute to a single Maximum-Quantum resonance (as in the DOSY chart). This feature strongly increases the resolving power of the technique, which has shown to be capable of distinguishing up to more than twenty molecular fragments with very similar NMR spectra. So far, MaxQ-NMR applications have focused on food chemistry (polyphenols) and environmentally relevant species (polyaromatic molecules). [22 23 24] Recently, an original feature

[a.] Aix Marseille Univ, CNRS, Centrale Marseille, iSm2, Marseille, France.
[b.] INRAE, Aix Marseille Univ, UMR1163 Biodiversité et Biotechnologie Fongiques, 13009, Marseille, France.
[c.] V. Mane Fils, 620 route de Grasse, 06620 Le Bar sur Loup, France.

View Article Online
DOI: 10.1039/D2AN00200K

of the technique has been explored to target already known molecules. Specifically, MaxQ-NMR can filter out the signal of several molecules, such as most of the cutting agents of seized illegal samples.[25] In this study, we go beyond exploring the application of 2D-MaxQ NMR and 3D-MaxQ-DOSY NMR to simplify the spectra of the enzymatic reaction mixtures. Two enzymatic systems were used as case study to assess this approach. The first system involved a fungal Copper Radical Alcohol Oxidase assisted by two accessory enzymes with 4-pyridinemethanol as substrate. In the second system, an oxidase, a ruthenium polypyridyl complex and a viologen are involved in the photo-catalytic oxidation of a styrene substrate to form three different products (epoxide, diol, aldehyde species). The Non-Uniform Sampling (NUS) acquisition accelerated the 2D and 3D experiments enabling to obtain spectra in 20 min and 3 hours, respectively.

Experimental

Samples under investigation

First system: 4-pyridinemethanol oxidation by a Copper Radical Alcohol Oxidase

Substrates, HRP type II and catalase from bovine liver were purchased from Sigma-Adrich (Germany). Molar concentrations of HRP and catalase were estimated by Bradford assay. The alcohol oxidase from *Colletotrichum graminicola* (*Cgr*AlcOx)[26] was recombinantly produced in bioreactor using *Pichia pastoris* X33 strain as host and purified by anion exchange chromatography as described previously.[27] Reactions were carried out in 4 mL-clear borosilicate glass vials closed by screw caps with PTFE septum for a total reaction volume of 500 µL. The reactions contained 10 mM substrate (prediluted in deuterated acetone), 1 µM *Cgr*AlcOx (corresponding to 50 µg/mL), deuterated sodium phosphate buffer (50 mM, pD 8.0), HRP at 12 µM and catalase at 0.5 µM final concentration (both enzymes were prediluted in D_2O). Final reaction contained 1 % (v/v) acetone. HRP is used to activate the *Cgr*AlcOx and catalase to remove the deleterious H_2O_2 generated during the catalytic cycle.[27] Reactions were run for 16 hours at 23°C, under shaking at 190 *rpm* in an Innova 42R incubator (New Brunswick, USA). Prior to NMR analysis, deuterated acetone was added up to 10 % (volume/volume) to enhance product solubilisation. The solutions were then transferred into 5 mm NMR tubes for successive NMR characterization. The *Cgr*AlcOx catalyses the oxidation of the alcohol to the corresponding aldehyde. Aldehydes are very unstable molecule and can react with other compounds to forms various products (*e.g.* hemiacetals). Furthermore, the 4-pyridinecarboxaldehyde is sensitive to hydration and is present in equilibrium with its *geminal*-diol form in aqueous medium.[28] The major expected products/intermediate are given in **Figure 1**.

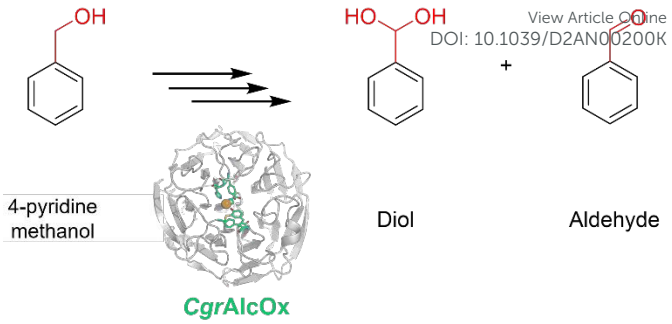

Figure 1 Predicted compounds of the first enzymatic system. The diol and aldehyde molecules correspond respectively to 4-pyridinecarboxaldehyde geminal-diol and to 4-pyridinecarboxaldehyde. *Cgr*AlcOx is the alcohol oxidase from *Colletotrichum graminicola.*

Second system: *p*-styrene sulfonate oxidation by a $[Ru(bpy)_3]^{2+}/MV^{2+}$/laccase/O^2 photocatlytic system

Substrates (Methyl viologen dichloride hydrate (MV), Sodium 4-vinylbenzenesulfonate (pSS), tris(bipyridine)ruthenium(II) chloride [Ru(bpy)3]2+) were purchased from Merck (Germany). The enzyme (a fungal laccase) was produced in a bioreactor using *Aspergillus niger* as host and purified from the broth by chromatography as previously described.[29] Molar concentration of LAC3 (86 kDa) was estimated by 610 nm absorption of T1 copper site. Reactions were carried out in 2 mL flat-bottom transparent glass HPLC vials closed by screw caps with PTFE septum. In the presence of 10 mM *p*-styrene sulfonate, 30 µM of each of $[Ru(bpy)_3]^{2+}$ (photo-catalyst), 4mM MV^{2+} (redox mediator) and 90 µM laccase (enzyme) were mixed in 100 mM air saturated B&R buffer pH 4.0. The photo-chemical reaction was operated under stirring on a flat white LED panel equipped with a Wratten 2B filter (λ>420 nm). *p*-styrene sulfonate (pSS) photo-oxidation kinetic was followed for 20 hours. The primary product is an epoxide that open spontaneously and forms a diol.[30] In the conditions of the experiment (i.e. dioxygen, sensitizer and light), an aldehyde may form through a dioxetane intermediate. The major expected products/intermediates are given in **Figure 2**.

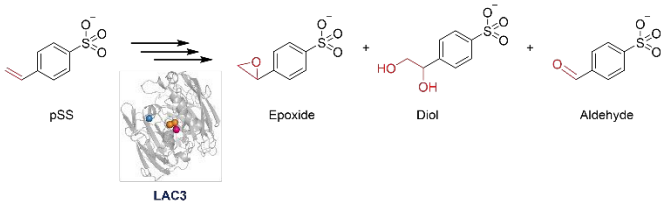

Figure 2 Compounds of the second enzymatic system. The epoxide, diol and aldehyde molecules are the products obtained by the photocatalytic reaction. LAC3 is the fungal laccase produced in a bioreactor using *Aspergillus niger* as host**.**

NMR recording conditions

All experiments were performed at 300 K on a Bruker Avance III spectrometer operating at 600 MHz for ^{1}H frequency equipped with an inverse triple resonance high-resolution probe producing pulse field gradients with a maximum strength of 60 G·cm^{-1}. All NMR data were processed with the TOPSPIN 3.2pl7 version software (Bruker BioSpin, Germany). MaxQ spectra (2D MQ/SQ correlation) were acquired with the standard sequence 90_x- $\tau/2$ -180_x- $\tau/2$ -$90_\phi - t_1 - 90_x$ - Aq **Figure 3.a**) described in details in previous works,[21 31 22] the coherence order (p) selection was carried out by two pulse field gradients (PFG) around the last 90deg pulse, by selecting the intensity of the second PFG equal to p times the first one. The interval $\tau/2$ was optimized to obtain the highest and uniform signal intensity, for the 4Q-1Q spectra. For the indirect dimension, 128 t_1 points with 16 scans were acquired. The relaxation delay was 2 s.

Standard DOSY spectra were recorded by a conventional convection compensated pulse sequence, based on the stimulated echo and incorporated bipolar gradient pulses and an Eddy current delay (BPP-LED).[1] The shape of all gradient pulses was Smoothed Square and the LED delay was of 5 ms. The diffusion delay Δ was set at 100 ms, the gradient strength, g, was linearly incremented in 32 steps from 2% to 98% of its maximum value with a duration of 1 ms, and 8 scans were recorded. Data were processed using DOSY Toolbox (GNU General Public License)[32] with 256 points. For the uniformly sampled (US) 3D MaxQDOSY-MaxQ experiment, the indirect MQ dimension was sampled with 128 increments leading to an experimental time of 2 days. To minimize the experiment time, we applied the Non-Uniformly Sampled (NUS) approach available on Topspin software, followed by Compressed Sensing (CS) reconstruction. The pulse sequence of the 3D MQDOSY-MQ experiment is reported in **Figure 3.b**.

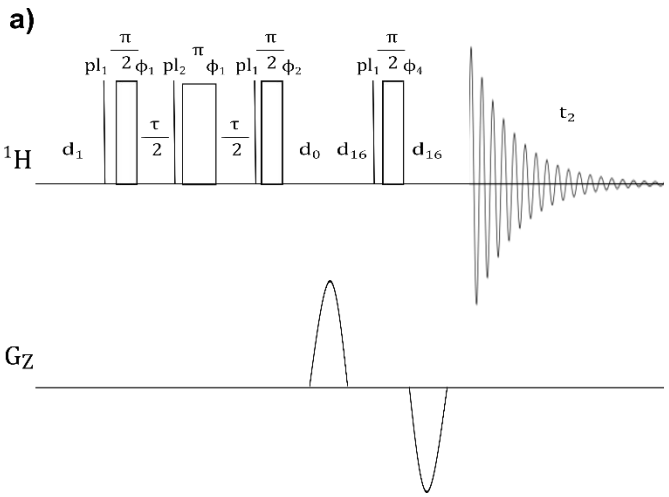

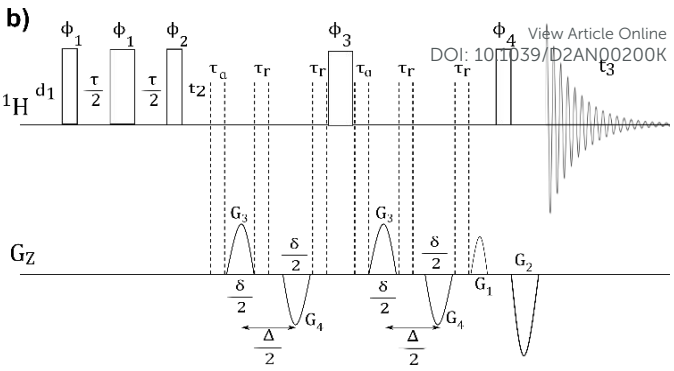

Figure 3 2D MaxQ pulse sequence **(a)**. 3D Convection compensated MaxQDOSY-MaxQ pulse sequence **(b).** Fine and large pulses represent RF pulse flip angles of π/2 and π, respectively. The ϕ_1 phase was equal to x, while ϕ_2 can be chosen to select odd or even MQ orders (x or y for even or odd order excitation, respectively), phases ϕ_2 and ϕ_3 can be fixed either on x or y. The duration of the preparation period τ was optimized to obtain as uniform as possible MQ excitation of the desired coherence order. The ratio of the coherence selection gradient pulses was chosen to fulfil G2 = p × G1, where p is the MQ coherence of choice (4 quanta in this study). τ_r are delays for gradient recovery times (about 200 µs) and τ_a equal to τ_r to center the π pulse.

Results and discussion

The 1D spectra of both reaction mixtures exhibit several signals in the aromatic regions. One can expect the presence of different compounds (intermediates, secondary products) in addition to the initial substrate and the product. For illustration, **Figure 4** depicts the quantitative 1D ^{1}H spectra of the reaction mixture of the *Cgr*AlcOx with its two accessory enzymes after 16 hours of reaction in the presence of 4-pyridinemethanol.

The ^{1}H MaxQ-NMR is a 2D experiment which isolate, in congested NMR spectra, the signals belonging to the same molecular fragments. Depending on the number of protons in the coupled spin system, the excitation of the highest coherence order (the maximum-quantum (MaxQ)) provides a singlet in the 'indirect' dimension correlating all peaks involved in this spin system. In this study, the substrates, 4-pyridinemethanol and p-styrene sulfonate, as well as the products and intermediates, illustrated in **Figure 1**, and **Figure 2** are di-substituted aromatic molecules, with a maximum excitable coherence of *4 quanta (p* = 4). Thus, the 4Q multiple quantum spectra would enable to isolate the peaks belonging to the different molecules.

View Article Online
DOI: 10.1039/D3AN00309K

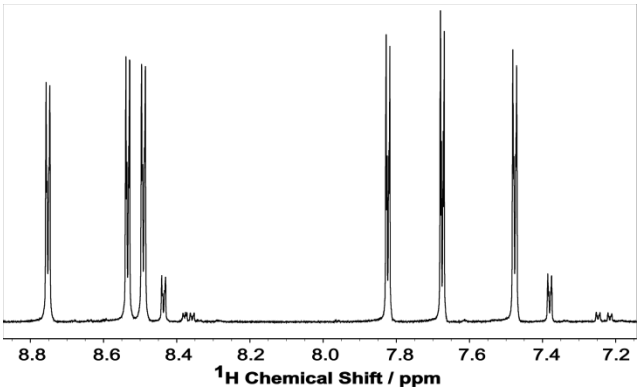

Figure 4 1D ^{1}H spectrum of the first enzyme system with the 4-pyridinemethanol as substrate, with a zoom in the region of 8.8-7.2 ppm.

One of the properties that made 1D NMR popular analytical technique is its quantitative response. Indeed, provided that the experiment is correctly parametrized (i.e., adequate relaxation delays to reach equilibrium of magnetization), the integral of NMR signal is proportional to the number of the observed nuclei. This direct relation is partially modified in nD spectra, where the multidimensional equivalent of the integral "the hypervolume element" becomes proportional to the transfer functions that consider all interactions that contribute to produce the n-dimensional cross-peaks (coupling, chemical shifts, relaxation… etc.), and depending on the timing and architecture of the pulse sequence. Since the extraction of quantitative information is one of the objectives, these parameters must be as homogeneous as possible.[33] Concerning the 2D MQ NMR, the multiple quantum coherences are typically excited using the pulse sequence depicted in **Figure 3a**. After the last ($\pi/2$) pulse, the amplitude of the antiphase terms produced by the coupling Hamiltonian is determined by the intensity of the selected coherence orders that are modulated by:[34]

$$2^{p}\prod_{i=2}^{p-1}\sin\left(\pi J_{ix}\tau\right) exp^{-\left(\frac{\tau}{T_{2i}^{*}}\right)} \quad (1)$$

Thus, the amplitude of the different coherence orders is strongly modulated by the main delay of the preparation period, τ.[i] In a spin system with different coupling constant J, the delay τ that provide the maximum intensity correspond to the reciprocal of the smaller coupling constant (J_{small}), $1/2J_{small}$. Theoretically, in aromatic spin system, this corresponds to J about 1 Hz, hence $\tau/2 = 0.5\ sec$. It has been shown that for free small molecules the sinusoidal dynamics along the τ delay is hampered by the exponential decrease due to the relaxation (T_2^*) and that $\tau/2$ around 0.3 ms is most often found as the optimal value.[34] However, this feature has never been assessed in the presence of large entities where the relaxation times decrease drastically. The evolution of the intensities of the 4Q signals as a function of the $\tau/2$ delay for the two pure substrates and the reaction mixtures are depicted in **Figure 5**. As expected, the evolutions in the presence of the enzymatic complexes are different from those of the free molecules.

According to equation (**1**) the sine evolution of the 4-quanta coherence intensity will be thwarted by the relaxation decay that leads to signal attenuation. The ideal and uniform excitation is rarely achieved because of this effect and a fair compromise is to get as close as possible to the optimal value to access to distant couplings without signal loss. For the free molecules (**Figure 5.c and Figure 5.d)** the second vertex of the sinusoid provides a relatively uniform excitation with the $\tau/2$ delay of 230 ms and 180 ms for the first and the second substrate, respectively. For the reaction mixtures (**Figure 5.a and Figure 5.b**) the relaxation decay is more manifest. However, for the first system **(Figure 5.a)**, the second vertex remains visible at $\tau/2 = 210\ ms$ unlike the second system (**Figure 5.b)** for which the only exploitable vertex is $\tau/2 = 55\ ms$.

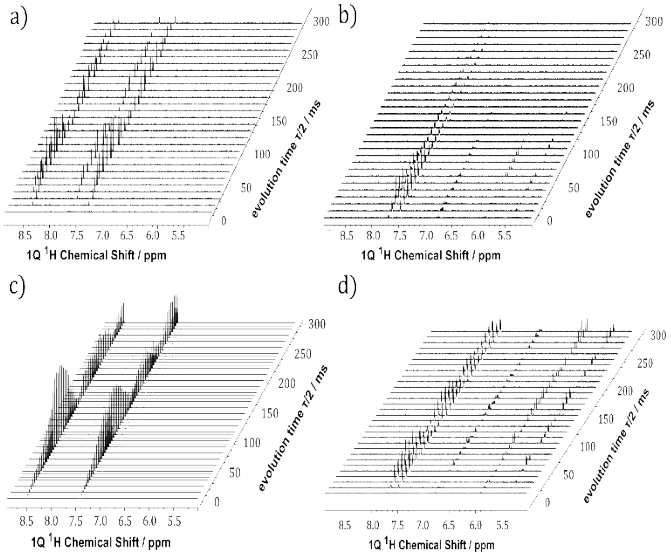

Figure 5 Evolution of the 4Q-filtered signals, displayed in absolute mode, of the reaction mixtures. **a)** first system with the enzyme, **b)** second system with the enzyme, **c)** first system only with the substrate, **d)** second system only with the substrate.

The interactions between the compounds and the large protein complexes, whether specific or not, lead to drastic reduction of the relaxation times. However, depending on the sample used, the behaviours are different. We retrieve the sinusoidal oscillation for the first system **(Figure 5.a)** but it is absent for the second where the relaxation contribution seems very important leading to a rapid extinction of the signal, probably due to the paramagnetic contribution from the multi-copper oxidase enzyme (laccase) as well as from the ruthenium photo-catalyst (**Figure 5.b**). From these observations, it is obvious that a standard implementation of MQ NMR cannot be envisaged to characterize the enzymatic reaction mixtures. The choice of the optimal preparation time, τ, should be guided visually for each sample.

Figure 6 depicts the 2D 4Q-1Q spectra for the two reaction mixtures obtained with the sequence described in **Figure 3.a**. These spectra provide a fingerprint in which the visual

enumeration of molecules is simplified since the peaks belonging to the same molecular fragments are aligned on the same frequency in the indirect dimension, and we can count six and four different components for the first and the second reaction mixture, respectively. Interestingly, when certain products or intermediates are present in low concentration they can be confused with ^{13}C satellites in the 1D ^{1}H spectra (see the F_2 projection in **Figure 6.b**). This ambiguity is resolved in the 2D MaxQ spectra where the satellites are filtered out.

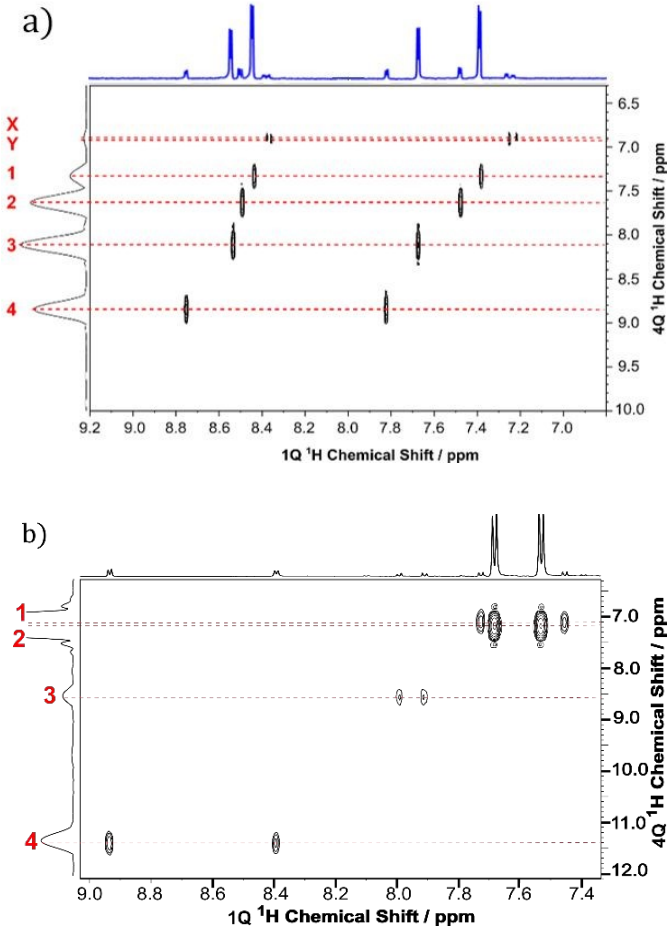

Figure 6 a) 2D 4Q-1Q spectrum of the first and **b)** the second complexes respectively, with a NUS at 25 % (a compression factor of 4) acquired with TD_1=128, NS=32 with a total experimental time of 30 minutes.

Acceleration and resolution improvement

For dynamic systems it is important to propose and carry out experiments with short acquisition times. To reduce the experiment time without information loss, we systematically applied the standard NUS acquisition procedure available with the Topspin software. It is known that the assessments of the correct NUS spectra reconstruction are qualitative and closely linked to the signal to noise ratios.[35] We did not resort to this visual evaluation, as this work has been widely carried out in the literature, and it is now admitted that a compression ratio of 4 allows producing faithful spectra in a reasonable experimental time without significant loss of resolution or signals, while avoiding artifacts. For each sample, the experiment time of the 2D 4Q-1Q was reduced to 34 min. Another application of the NUS acquisition procedure is to increase the resolution in the indirect dimension without experiment time cost by increasing the number of points in the indirect dimension with a factor equal to the compression rate. **Figure 7** shows the NUS 2D 4Q-1Q spectrum of the laccase reaction mixture (second experimental system) recorded with 256 points in F1 and a compression rate of 4. This results in an increased resolution of the two peaks around 6 ppm in the indirect dimension. However, some compression artifacts appear (red circle).

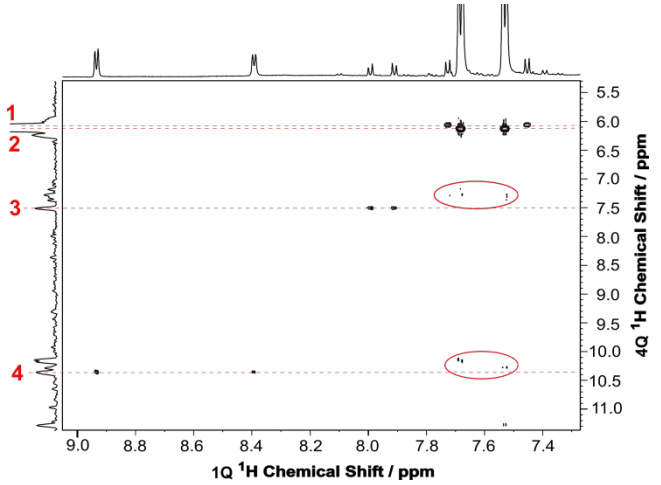

Figure 7 2D 4Q-1Q NUS (25%) of the second system using 256 points (TD1) in the indirect dimension, obtained in 48 minutes. Standard experiment time is 3.25 hours. Compression artefacts are showed inside the red circles.

An important property of the MaxQ experiment, which is not explicit in the literature, is highlighted in this section. It concerns the dependence of chemical shifts in the indirect dimension (MaxQ) on the carrier frequency. Indeed, the deviation from the carrier frequency in the indirect dimension is equal to the sum of the deviations from the carrier frequency of the peaks participating to the MaxQ transition, which can be expressed as follows:

$$\delta_{maxQ}^{ppm} - O_1^{ppm} = \sum_{i=1}^{p} \left(\delta_i^{1Q} - O_1^{ppm}\right) \quad (2)$$

Where δ_{maxQ}^{ppm} is the MaxQ chemical shift in the indirect dimension, O_1^{ppm} the carrier frequency in *ppm*, δ_i^{1Q} and *p* are the 1Q chemical shifts and the number of the protons (also the coherence order) participating to the MaxQ transition, respectively. In **figure 6b**, the O_1^{ppm} was *7.75 ppm*, and in **figure 7**, O_1^{ppm} was *8.10 ppm*. As a consequence, the chemical shifts in the indirect dimension are different. This feature must be considered to predict the correct chemical shifts in the MaxQ dimension. Finally, a last subtility concerns the equivalent protons, as is the case here with the di-substituted aromatic molecules, the contribution of two protons for

View Article Online
DOI: 10.1039/D2AN00269K

each chemical shift must be considered for the calculation of the chemical shift in the indirect dimension.

2D DOSY and 3D MaxQ-DOSY

The effectiveness of DOSY NMR for a direct identification of the mixture composition are well established.[12] [13] Provided that both mobility and spectral resolution are sufficient, it allows the extraction of NMR spectra of pure compounds. On the other hand, the resolving power of DOSY has been limited by technical and signal processing difficulties. Indeed, much of the research in the development of better DOSY experiments focuses on this latter aspect. When numbering purpose is sought during a first analysis step, DOSY NMR can also be an appropriate method. We explore this feature in this section. The DOSY spectrum of the *Cgr*AlcOx reaction mixture obtained using the standard convection compensated pulse sequence, with the parameters given in experimental section, is presented in **Figure 8.** The first interesting feature that can be highlighted is the non-expected resolution due to mobility which is sufficient to allow detecting the six compounds and extracting their diffusion coefficient. Given the identical molecular size of these compounds which have only undergone chemical modifications of the main functions (alcohol - aldehyde- acid-....), the diffusion coefficients should be very close and would not allow isolating the compounds. The only entity presents in the mixture which can affect the diffusion coefficients in a different way is the protein complex which can differentially interact with the compounds according to the affinity. However, the diffusion coefficients of the molecules 2 and 3 are similar and not resolved with the standard Inverse Laplace transform.

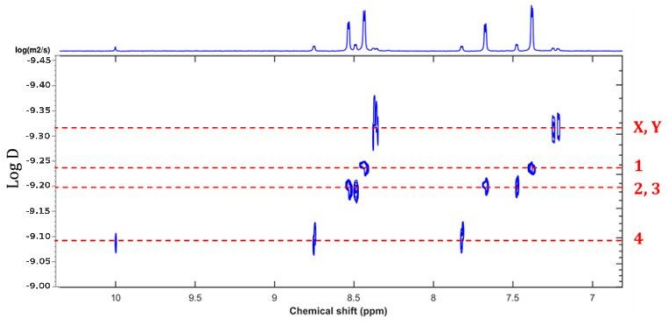

Figure 8 2D DOSY spectrum for the first system using a standard convection compensated pulse sequence (Bruker notation: dstebpgp3s). Processed with DOSY Toolbox (GNU General Public License) with 512 points.[32]

Assuming that the observed difference in diffusion comes from the interaction with the enzyme, one can extract the diffusion coefficients and classify the molecules according to their relative affinities for the first enzymatic complex, in descending order: X,Y / 1 / 2,3 / 4.

Several three-dimensional NMR sequences have been proposed to increase the spectral resolution of DOSY through a third dimension to further spread out overlapping resonances.[19] [17] [36] [16] Recently, we developed 3D MaxQ-DOSY that associates the two "*demixing*" power of each method (MaxQ and DOSY) and offers a more simplified layout.[37] The 3D 4Q-DOSY spectrum and its three 2D projections are reported in **Figure 9.** 4Q-DOSY means that the diffusion effect was encoded while the 4Q coherence order was excited, which was also the MaxQ order for the six molecules within the reaction mixture. To compensate the increased sensitivity to magnetic field gradients because of effective gyromagnetic ratios ($p\gamma$), the gradient pulse duration δ was divided by p. Doing so, a better resolution is provided especially in the 4QDOSY-4Q projection plane with only one spot par molecule located at the crossing of the value of the translational molecular diffusion and the MaxQ (4Q) chemical shift, δ_{MaxQ}. However, the two least concentrated compounds, previously noted X and Y, are not detected, due to a low sensitivity that need a longer experiment. The duration of the 3D experiments is a drawback. For this reason, we collected data from this experiment with the Non-Uniform Sampling (NUS) with a compression factor of 4 (25 %), leading to an experiment time of 3 hours.

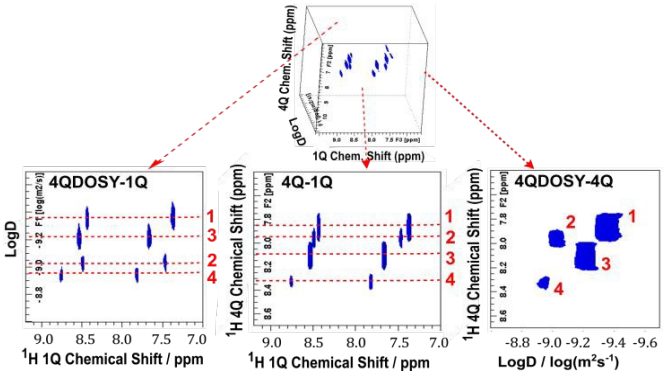

Figure 9 Projections of the zoom of the 4QDOSY-4Q 3D experiment in the region of 9.5-7 ppm for the first enzyme system. Left: 4QDOSY-1Q projection; middle: 4Q-1Q projection; right: 4QDOSY-4Q projection. The scale in the 4Q dimension corresponds to a normalization to the p-quantum order (a division by 4 in this case).

It is important to note that the Inverse Laplace Transform (ILT) of the 3D experiment leads to a different result from the standard 2D-DOSY chart. Indeed, the diffusion coefficient of compounds 2 and 3 in **Figure 8** is substantially the same, whereas in the ***4QDOSY-1Q*** projection of the 3D experiment (**Figure 9**), the diffusion coefficient of compound 2 is different from 3 and is closer to that of compound 4. We are not able to fully explain this difference, but we can consider that two aspects can add up, the first concerns the convection effects that are amplified in the 3D MaxQ-DOSY experiment by the effective gyromagnetic ratio ($p\gamma$), and are not completely compensated, especially when high quantum orders (4Q in this study, p=4) are selected. The second may be due to the ILT processing which may not be suitable for the maxQ-DOSY

experiment, this point should be studied later. In this study, we show the capability of the sequence to provide an extreme simplification, one peak by molecule in the 4QDOSY-4Q projection (**Figure 9**), but currently it cannot be used quantitatively. Indeed, from the 3D data, by fitting the evolution of the intensity of the 2D-MaxQ cross peaks as a function of the gradients strength, we extract almost the same diffusion coefficients as those obtained with the standard 2D DOSY, hence the projection ***4QDOSY-1Q*** does not reflect the true diffusion coefficients. **Table 1** compare the diffusion coefficients obtained from the DOSY projections and from the fitting procedures.

Table 1. Diffusion coefficients ($m^2.s^{-1}$) for the four major compounds obtained from the DOSY projections of **Figures 8** and **9**, and by fitting the data of the 2D and 3D experiments.

	comp 1	Comp 2	Comp 3	Comp 4
2D-DOSY **Fig. 8**	5.78 10^{-10}	6.32 10^{-10}	6.32 10^{-10}	8.11 10^{-10}
2D-DOSY **Fit**	5.95 10^{-10}	7.08 10^{-10}	6.71 10^{-10}	8.31 10^{-10}
3D-DOSY **Fig. 9**	4.41 10^{-10}	9.44 10^{-10}	5.95 10^{-10}	11.22 10^{-10}
3D-DOSY **Fit**	6.00 10^{-10}	6.6 10^{-10}	7.23 10^{-10}	9.10 10^{-10}

It is obvious that DOSY charts can be used qualitatively to analyse the mixture. However, the 3D MaxQ-DOSY should not be used to exploit the diffusion coefficients to extract conclusions on the affinity, as the order was changed from the 2D DOSY. It would nevertheless allow a qualitative analysis and greatly improve the resolution in more complex systems. At last, as shown in **Figure 8**, the spread in the dimension of the diffusion does not allow a precise determination of the diffusion coefficients. For a quantitative analyse, the accurate diffusion coefficients are obtained by fitting the data from the 2D-DOSY experiment.

Conclusions

In summary, we showed that the NMR spectra of mixtures resulting from the reaction of enzyme complexes can be simplified using the well-established 2D Maximum Quantum NMR approach, which allows rapid counting of molecules by isolating the peaks belonging to the same component. For quantification purpose, the simple approach that can be envisaged is to return to the 1D proton spectra to perform the integration of the identified peaks. In the case of a mixtures of free small molecules, the delay of the preparation period, τ, of the Multiple Quantum pumping block of 500 ms is accessible. This parameter becomes very limiting when compounds are interacting with large entities and even more, when paramagnetic elements are present. Depending on the studied system, the reduction of the relaxation times implies an adjustment to find a compromise between a uniform excitation and a loss of the signal, respectively 110 and 420 ms for the studied systems. This approach can be easily transposed to more complex systems with significant overlaps or with broad peaks. Indeed, MQ-NMR experiment has been shown to be able to decompose very crowded spectra, and is insensitive to peak overlaps. Recent developments with the NUS recording approach enable to acquire 2D MQ spectra with short experimental times appropriate to fragile and unstable systems. Finally, the association of the MaxQ and diffusion spectroscopy represent an interesting combination that provide an extreme simplification of NMR spectra and allow to access to valuable information as the molecular interactions. This association will probably pave the way for other applications and methodological developments for its improvement in terms of sensitivity and fast acquisition.

Conflicts of interest

There are no conflicts to declare.

Acknowledgements

- The project leading to this publication has received funding from the Excellence Initiative of Aix-Marseille University – A*Midex foundation, a French "Investissements d'Avenir" program, for the Ph.D. fellowship of E.P.
- This study was also supported by the French National Agency for Research ("Agence Nationale de la Recherche") through the ANR-NSERC "FUNTASTIC project", ANR-17-CE07-0047. We are grateful to MANE & Fils and the "Association Nationale Recherche Technologie" (ANRT) for funding the PhD fellowship of D.R. This Convention Industrielle de Formation par la RecherchE (CIFRE) grant no. 2017/1169 runs from 1 April 2018 to 1 July 2021.
- We thank Elise Courvoisier-Dezord from the Plateforme AVB (AMU): Analyse et Valorisation de la Biodiversité and Yolande Charmasson for help in the production of recombinant laccases.

Notes and references

1 J. E. Tanner, *The Journal of Chemical Physics*, 1970, **52**, 2523–2526.
2 J. J. Eicher, 2012, 26.
3 D. A. Blass and E. Adams, 10.
4 J. Ma, S. McLeod, K. MacCormack, S. Sriram, N. Gao, A. L. Breeze and J. Hu, *Angew. Chem. Int. Ed.*, 2014, **53**, 2130–2133.
5 R. M. Werner and A. Johnson, *Biochem. Mol. Biol. Educ.*, 2017, **45**, 509–514.
6 F. Exnowitz, B. Meyer and T. Hackl, *Biochimica et Biophysica Acta (BBA) - Proteins and Proteomics*, 2012, **1824**, 443–449.
7 J. D. Kehlbeck, C. C. Slack, M. T. Turnbull and S. J. Kohler, *J. Chem. Educ.*, 2014, 5.
8 Y. Jiang, T. McKinnon, J. Varatharajan, J. Glushka, J. H. Prestegard, A. T. Sornborger, H.-B. Schüttler and M. Bar-Peled, *Biophysical Journal*, 2010, **99**, 2318–2326.
9 Peter. Stilbs, *Anal. Chem.*, 1981, **53**, 2135–2137.

View Article Online
DOI: 10.1039/D2AN00200K

10 E. O. Stejskal and J. E. Tanner, *The Journal of Chemical Physics*, 1965, **42**, 288–292.
11 P. Stilbs, *Progress in Nuclear Magnetic Resonance Spectroscopy*, 1987, **19**, 1–45.
12 K. F. Morris and C. S. Johnson, *J. Am. Chem. Soc.*, 1992, **114**, 3139–3141.
13 K. F. Morris, Peter. Stilbs and C. S. Johnson, *Anal. Chem.*, 1994, **66**, 211–215.
14 H. Barjat, G. A. Gilles, S. Smart, A. G. Swanson and S. C. R. Williams, *J. Magn. Reson.*, 1995, 170–172.
15 B. Antalek, *Concepts in Magnetic Resonance Part A*, 17.
16 S. Viel and S. Caldarelli, *Chem. Commun.*, 2008, 2013.
17 M. Nilsson, A. M. Gil, I. Delgadillo and G. A. Morris, 5.
18 M. Nilsson and G. A. Morris, *Journal of Magnetic Resonance*, 2005, **177**, 203–211.
19 D. Wu, A. Chen and C. S. Johnson, 4.
20 A. Jerschow and N. Müller, *Journal of Magnetic Resonance, Series A*, 1996, **123**, 222–225.
21 M. R. G. N. and S. Caldarelli, *Anal. Chem.*, 2010, **82**, 3266–3269.
22 G. N. M. Reddy and S. Caldarelli, 2011, 3.
23 A. Wokaun and R. R. Ernst, *MOLECULAR PHYSICS*, 1978, 317–341.
24 G. N. M. Reddy and S. Caldarelli, *Analyst*, 2012, **137**, 741–746.
25 M. Yemloul, I. M. Adyatmika, S. Caldarelli, D. Ollivier and M. Campredon, *Anal Bioanal Chem*, 2018, **410**, 5237–5244.
26 S. Urresti, M. Lafond, E. M. Johnston, F. Derikvand, L. Ciano, J.-G. Berrin, B. Henrissat, P. H. Walton, G. J. Davies and H. Brumer, *NATURE COMMUNICATIONS*, 13.
27 D. Ribeaucourt, B. Bissaro, V. Guallar, M. Yemloul, M. Haon, S. Grisel, V. Alphand, H. Brumer, F. Lambert, J.-G. Berrin and M. Lafond, *ACS Sustainable Chem. Eng.*, 2021, **9**, 4411–4421.
28 F. Crespi, D. Vega, A. K. Chattah, G. A. Monti, G. Y. Buldain and J. M. Laz, *J. Phys. Chem. A*, 2016, 8.
29 Y. Mekmouche, S. Zhou, A. M. Cusano, E. Record, A. Lomascolo, V. Robert, A. J. Simaan, P. Rousselot-Pailley, S. Ullah, F. Chaspoul and T. Tron, *Journal of Bioscience and Bioengineering*, 2014, **117**, 25–27.
30 L. Schneider, Y. Mekmouche, P. Rousselot-Pailley, A. J. Simaan, V. Robert, M. Réglier, A. Aukauloo and T. Tron, *ChemSusChem*, 2015, **8**, 3048–3051.
31 A. Bax, P. G. De Jong, A. F. Mehlkopf and J. Smidt, *CHEMICAL PHYSICS LETTERS*, 1980, 567–570.
32 M. Nilsson, *Journal of Magnetic Resonance*, 2009, **200**, 296–302.
33 S. Heikkinen, M. M. Toikka, P. T. Karhunen and I. A. Kilpeläinen, *J. Am. Chem. Soc.*, 2003, **125**, 4362–4367.
34 G. N. Manjunatha Reddy and S. Caldarelli, *Magn. Reson. Chem.*, 2013, **51**, 240–244.
35 A. Le Guennec, J.-N. Dumez, P. Giraudeau and S. Caldarelli, *Magn. Reson. Chem.*, 2015, **53**, 913–920.
36 E. K. Gozansky and D. G. Gorenstein, *Journal of Magnetic Resonance, Series B*, 1996, **111**, 94–96.
37 G. N. Manjunatha Reddy, M. Yemloul and S. Caldarelli, *Magn. Reson. Chem.*, 2017, **55**, 492–497.